Size, Concentration and Content Effect of Copper/Graphite Hybrid Dopant on Mechanical, Thermal and Electrical Conductivity Characteristics of Unsaturated Polyester Resin

K. Yaman[a,*] and M. Fatih Öktem[b]

[a]The Scientific and Technological Research Council of Turkey,
Defense Industries Research and Development Institute, 06261, Ankara, Turkey

[b]Ankara Yıldırım Beyazit University, Depth. of Metallurgy and Materials Eng., 06010, Ankara, Turkey

(Received August 22, 2019; revised version December 6, 2019; in final form December 23, 2019)

In this paper, mechanical, thermal, electrical, and physical properties of unsaturated polyester resin with dendritic-shaped copper(Cu)-graphite (Gr) fillers were experimentally investigated and correlations were proposed with several theoretical models. On the other hand, the Gr filler is added as a secondary filler to provide synergy and obtain better conductivities. For this purpose, 5 wt% Gr filler was added as a secondary filler while Cu was added with changing weight rates. In each experiment, the basic aim is to determine the effects of both filler size and concentration on the mechanical, thermal, and electrical characterizations of the composite mixture. It is observed that an increase in filler concentration causes an increase in thermal conductivities. On the contrary, the coefficient of thermal expansion and specific heat decrease with increasing filler content. The hybrid filler allows the positive synergistic effect on mechanical performance but restricts conductivity properties. The particle size also causes a minimal linear increase in thermal conductivity. Thermal analysis such as thermogravimetric analysis and differential scanning calorimetry show that the thermal stability increases with the filler concentration. On the other hand, the electrical conductivity increases with increasing filler particle size and concentration. Using this high conductive novel composite mixture as an electrode hard steel parts were engraved in an electric discharge machine. Regarding the experimental-theoretical correlation, the best agreement is achieved with the Maxwell model.

DOI: 10.12693/APhysPolA.137.339

PACS/topics: thermal conductivity, polymer composite, hybrid filler, dendritic shape, electrical conductivity

1. Introduction

Several studies have examined the addition of non-polymeric fillers to improve the physical properties of polymer-based composites. Doping of fillers with good mechanical, thermal, and electrical properties improves the composite material relatively to pure resin but never reaches the level of pure filler. Besides, the composite mixture in a viscous form can easily be shaped by pouring into a mold before curing. Due to the ability to be shaped easily, complex geometries can be produced with this method.

On the other hand, the addition of more than one filler may create the possibility of interaction between the particles. These interactions provide synergy to obtain better properties. In this paper, the basic motivation is to achieve the effects of particle size and concentration of dendritic-shaped Cu particles as primary filler and Gr as secondary filler on mechanical, thermal, and electrical conductivity characteristics. In order to examine the synergistic effect, Gr particles have been added to the present mixture with a fixed 5 wt%. In this work a novel composite structure was investigated in terms of material composition and powder size.

In a study made by Zhou et al., researchers investigated both thermal and electrical conductivities of filler doped polymers [1]. They reported that the thermal and electrical conductivities are related to the filler shape and size as well as the added filler concentration. At high filler loadings, the thermal and electrical conductivities increased remarkably. On the contrary, i.e., in lower filler loadings, particles of conductive material encapsulated by a polymer binding cannot touch each other. Insulation between particles leads to lower electrical conductivity [1, 2]. Under constant particle concentration [3], particle sizes were compared. The results show that higher thermal conductivity λ is achieved with greater particle size. Ren et al. [4] observed the effect of filler shape on thermal conductivity (TC) by using optical microscopy, atomic force microscopy, and scanning electron microscopy, respectively. They showed that the networks of thermally conductive fillers and the interfacial thermal resistance at the filler boundaries played a major role in the TC. Boron nitride particle (BNp) exhibits the higher TC than boron nitride sheet (BNs) in the polyethylene

*corresponding author; e-mail: kemal.yaman@tubitak.gov.tr

media. However, the addition of multi wall carbon nanotube (MWCNT) as hybrid component reversed this situation. The TC of the hybrid BNs is superior to that of the hybrid BNp composites. The comparisons showed that the TCs are larger than Maxwell and Bruggeman models for both 2-phase and 3-phase composite structures. In another study made by Yuan et al. [5], tetrapod-shaped zinc oxide (T-ZnO) whiskers and boron nitride (BN) flakes were employed to improve the thermal conductivity of phenolic formaldehyde resin. They have observed that the addition of BN flakes increased the TC and flexural properties. Yu et al. [6] also investigated the effect of filler morphology. They assert that the prolate-shape filler can improve the TC by forming conductive network.

In hybrid systems, Zhang et al. [7] used two different dimensional fillers to explore their synergistic effect on the mechanical and electrical properties of PMMA composite. They reported that the hybrid filler promotes the mechanical performance but restricts the synergistic effect for electrical properties. In the study of Sharmila et al. [8] graphene oxide and iron oxide hybrid filler epoxy binder composite are investigated for mechanical, thermal, and dielectric properties. Scanning electron microscopy (SEM) and transmission electron microscopy (TEM) analysis showed that the adhesion between the hybrid filler and the epoxy matrix is quite strong. Hybrid structure also exhibited higher thermal stability than the neat epoxy resin. Dielectric properties like dielectric constant and dielectric loss increased with increase in hybrid filler content. In another work [9] hexagonal boron nitride (hBN) platelets and aluminum nitride (AlN) particles are used as hybrid fillers to improve the thermal conductivity of polytetrafluoroethylene (PTFE). The Hashin–Shtrikman model is also used to quantify the filler connectivity within polymer matrix. The incorporation of hybrid fillers improves the thermal stability of PTFE matrix and PTFE composites retain dielectric properties.

As can be seen from the literature, the theoretical models have been widely used to simulate the electrical and thermal behavior of the composite materials without testing. The basis of many of them is the Maxwell model [1, 10–16]. The Hashin–Shtrikman [10] and the Lewis–Nielsen [1, 2, 10–17] models are also investigated. For 3-phase system Lewis–Nielsen model has been extended as modified Lewis-Nielsen model and provides good convergence with the experimental hybrid systems [18–20]. Badakhsh and Park [19] investigated the thermal and mechanical properties of high-density polyethylene (HDPE)-matrix reinforced copper-carbon nanotube filler composite. Characterization results indicate the increase in TC and reduction in thermal expansion. For EC of three or more phase composite structures, the Bruggeman symmetrical effective medium theory [21], which is based on the spherical filler shape, gives the more accurate prediction. Hence, we also used the same approach to predict the EC values. The comparison between the theoretical models and experimental results proposed in this work is reported. In the whole text, copper–polyester composite is denoted by C/P and copper–graphite–polyester hybrid composite is denoted by C/G/P.

2. Experimental

Copper and graphite powder have been sieved into ten different size groups to investigate the effect of particle size on thermal properties. The powder particle sizes and distributions have been carried out on a measuring instrument (MASTERSIZER-X, Malvern Inst., Worcestershire, UK) using the laser light diffraction method. The particle size distributions of Cu/Gr are shown in Fig. 1. The average grain sizes are 75 μm for Cu and 70 μm for Gr. The UPR including 35±2% styrene as a reactive diluent, with brand name CE 92-N8, were obtained from Cam Elyaf Co. (Turkey). Cobalt and methyl-ethyl-ketone peroxide were used, respectively, as additives to accelerate and initiate the curing of the composite mixtures. They were obtained from Akzo-Nobel Co. (Turkey Dist.). In Table I the properties of pure UPR are given by Cam Elyaf Co.

The composite specimens were prepared by mixing a 30 ± 1 cm^3 resin/filler mixture for 15 min at an angular speed of 50 ± 10 rpm using a mechanical mixer. During this process 1.5 ± 0.1 g of the accelerator catalyst was added at the specified ratios. The 5 ± 0.2 g of hardener was added, and next the mixture was stirred for further 5 min. In this way, the fluidized mixture is poured into the mold without hardening. After pouring, the mixture stayed for 15 min for pre-curing. The pre-cured specimens are post-cured at a temperature of $150 \pm 2\,^{\circ}$C for 4 h. The same procedure was applied for fixed 5 wt% Gr filler [22]. The hardened specimens were formed into discs with 20±0.2 mm diameter and 8±0.1 mm thickness. The coefficient of thermal conductivities λ were measured

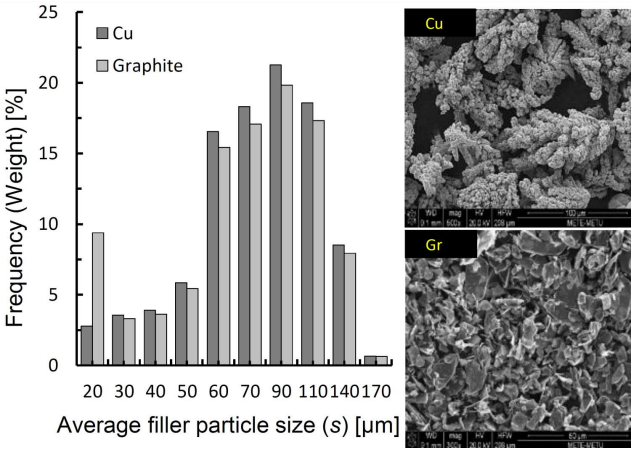

Fig. 1. Cu and Gr filler SEM images and their particle size distribution.

TABLE I

Properties of UPR [22].

Physical properties	
viscosity [cps]	600-700
monomer [%]	Styrene 35 ± 2
acid No. [mg/KOH/g]	28 ± 2
density [kg/m^3]	1200 ± 10
Hardening characteristics	
gelling time [min]	7 ± 2
peak temperature [°C]	150 ± 5
peak temperature duration time [min]	12
total peak temp reach time [min]	20
Mechanical properties	
microhardness [HV]	18.62
elongation at break [%]	20
tensile stress [MPa]	45.26
tensile modulus [GPa]	1.177

TABLE II

Material properties of composite component [22], including density ρ, average particle size d, melting temperature T_m, and thermal conductivity λ.

Properties	UPR	Cu filler	Gr filler
d [μm]	–	$75 \pm 5\%$	$70 \pm 4\%$
ρ [kg/m^3]	1200 ± 10	8920	2200
T_m [°C]	280	1084.6	900
λ [W/(m K)]	0.22 ± 0.02	385 ± 5	120 ± 2

by a C-Therm TCI model thermal conductivity analyzer. The modified transient plane source technique was used to characterize the λ and effusivity of composite materials. The measurements were carried out at 24 °C with a flat probe having 17 mm diameter. TGA was performed with a HITACHI TG/DTA 6300 thermo-gravimetric analyzer. DSC analysis was performed with a HITACHI DSC7020 analyzer under nitrogen atmosphere. When heating samples at a rate of 10 °C min^{-1} from room temperature up to 700 °C, we were able to trace the mass loss. The morphology of the inner state of composites was examined by SEM technique. The particle size group and physical properties of the components that form the composite structure, are given in Fig. 1 and Table II, respectively. Coefficients of thermal expansions (CTE) were measured using a thermal expansion/shrinkage analyzer (LINSEIS L75 vertical bench model dilatometer with ΔL±0.3 nm resolution). Those samples having 6 ± 0.1 mm in diameter and 20 ± 0.2 mm in length were heated up to 150 °C at a rate of 10 °C per minute and then measurements were taken.

The values of λ were determined from the slope of the plot at 60 °C and 150 °C. Electrical resistance was measured with a KEITHLEY-619 DC electrometer in a range of $(0.1–2.0) \times 10^{12}$ $\Omega \pm$ (10% rdg+10 counts) using two-point contact method [23, 24]. The sample was disc-shaped with a diameter of 15 ± 0.2 mm and a thickness of 2 ± 0.1 mm. In addition, tensile tests were applied in order to see the effect of hybrid filler on mechanical performance. These tests were carried out at temperature of 23 °C and a strain rate of 2 mm/min tensile speed by using a micro-controlled universal testing machine (model WDW 50 E).

3. Results and discussion

This section consists of five subsections, namely, mechanical, thermal conductivity, thermal expansion, density, specific heat, and electrical conductivity. The results of experimental work in each section are presented. At first, the thermal stability characterization of composite mixture is investigated. The Cu content increases the thermal stability of UPR alone. This may be explained by the lower heat capacity and higher λ of Cu–Gr mixture, which causes dissipation of the heat. This will result in polyester chains starting to degrade at higher temperatures [25–27].

The resin curve by TGA (shown in Fig. 2a) indicates that the value of the temperature at which the first loss of weight occurs is about 250 °C. For almost all polymer composites, the weight loss has ended at about 420 °C. Compared to neat resin the TGA shows the significant weight loss at about the interval of 13–25%. The DSC of C/G/P composites for three different filler loadings are given in Fig. 2b. The change in decomposition is clearly observed. The maximum weight loss occurs at the temperature interval of $\sim$ 300–400 °C. The DSC shows that the thermal stability is increased by the filler concentration [25–28]. It can also be said that the degradation in the composite structure is proportional to the thermal resistance. Therefore, the thermal resistance decreases with decreasing degradation by addition of the filler material. The perfection of the crystalline regions of pure UPR is destroyed by the interaction between the pure UPR and the Cu filler. It can also be said that filler particles may cause a more significant effect on crystallinity as the filler concentration is increased [26, 29].

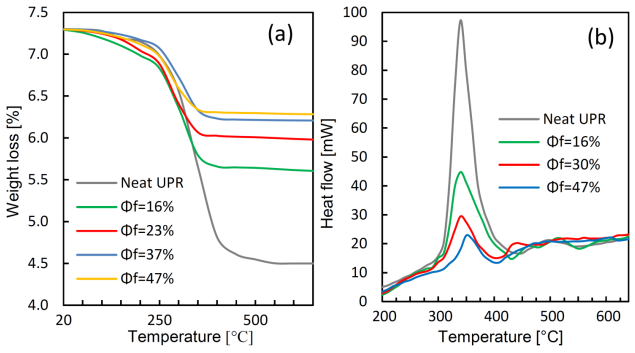

Fig. 2. (a) TGA and (b) DSC curves of C/G/P for different volumetric concentrations of Cu.

3.1. Mechanical

In order to investigate the effect of hybrid system on mechanical performance, the tensile tests were carried out and the obtained results were given in Fig. 3 as tensile stress–strain curves and Young's moduli. The hybrid system is composed of 75 wt% Cu (volumetric Cu ~ 30%), of 5 wt% Gr, and 20 wt% resin. It was observed that the hybrid structure increased tensile strength compared to copper doped composite and neat resin and had a positive synergistic effect on the composite structure. It was also seen that hybrid specimens break at higher tensile values than copper doped specimens alone. Similar results are given in the literature [5, 7, 8, 19].

3.2. Thermal conductivity λ

The experimental thermal conductivity values of the Cu/polyester (C/P) and Cu/Gr/polyester (C/G/P) composites with increasing filler loadings are shown and comparisons of the theoretical models are given in Fig. 4. The Maxwell model gives the closest values to the experimental results. Meanwhile, both the theoretical and the experimental values indicate that λ increases with the filler concentration [1–3, 10–16]. Generally, the experimental λ values are higher than that of the given theoretical models (see literature [1, 10, 11, 13]).

In this work, C/P and C/G/P conductivity results, on the one hand, appear below the Maxwell model results, and on the other hand, above the results of Hashin–Shtrikman and Lewis–Nielsen (Fig. 4). Our results show also that the addition of Cu into the matrix increased the λ more than 20 times that of neat unsaturated polyester resin (UPR). However, the Gr addition as hybrid filler did not give the expected synergistic effect. The addition of Gr particles to the solution reduces the concentration of Cu filler, which has much higher thermal and electrical conductivities than that of Gr. Especially at higher Cu filler loading, Gr particles decrease the wettability and dispersion of Cu particles in matrix media. These low wetting and dispersion effects result in an interface thermal resistance between the thermally conductive particles. When Gr particles are added, the area of the interface per unit volume greatly increases. This increase, in turn, causes the scattering of heat carriers (i.e., phonons). They occur at the interface between the two environments, and this weakens the conduction of heat [30]. Finally, the addition of Gr particles as hybrid fillers shows that the spatial distribution of the particles in the matrix medium has a pronounced effect on TC. Similar results were obtained in [7–9, 18, 30, 31]. Note that the composite mixture saturates only at a volumetric concentration of about 60% when only Cu is added. The Gr content decreases then by as much as 48%, since no more Cu powder dissolved in UPR resin for the given condition (24 °C at room temperature and microscale filler size). On the other hand, the addition of Gr into the mixture increases the mechanical performance and dielectric property of composite structure.

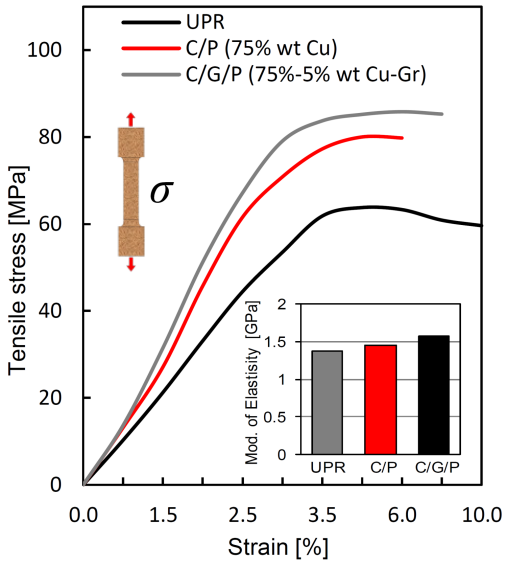

Fig. 3. Tensile test results for neat resin, C/P, and hybrid composites.

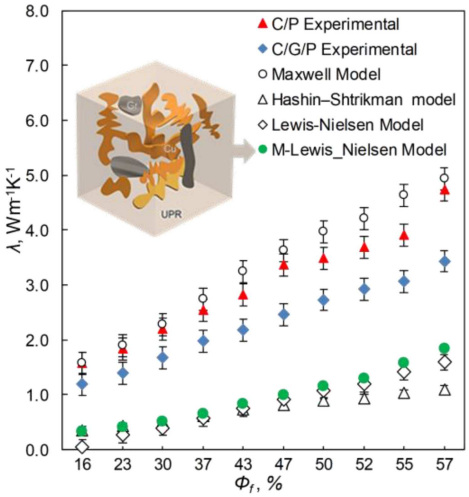

Fig. 4. Variation of λ of 3-phase composite system vs. filler content and comparison of the theoretical models.

In this study, as Gr wt% is constant and relatively small and Cu filler wt% is varying, the composed structure is assumed as 2-phase structure. The Maxwell, Hashin–Shtrikman, and Lewis–Nielsen models were used in the theoretical calculations. The Maxwell model is limited to single filler component and hence more than one filler was used in this study, and Lewis–Nielsen model is used [31]. However, the most frequently used model in the literature for 3-phase systems is modified Lewis–Nielsen approach. It is described by

$$\lambda_c = \left(\frac{1 + \sum_{i=1}^{n} AB_i \Phi_i}{1 - \sum_{i=1}^{n} B_i \Psi_i \Phi_i} \right) \lambda_m, \tag{1}$$

$$B_i = \frac{\frac{\lambda_{fi}}{\lambda_m} - 1}{\frac{\lambda_{fi}}{\lambda_m} + A}, \tag{2}$$

$$\Psi_i \cong 1 + \frac{\Phi_i}{\Phi_{mp}} \left(\Phi_{mp} \Phi_i + (1 - \Phi_{mp}) \Phi_i \right), \tag{3}$$

where $i \in \{1, 2\}$, λ_{fi} is the thermal conductivity of the i-th filler component (i.e., λ_{f1} for filler1 and λ_{f2} for filler2), λ_m is TC of matrix resin, and Φ_i is the volume fraction of the i-th filler component. Calculations with the use of Eqs. (1)–(3) are shown in Fig. 4 as M–Lewis–Nielsen model [18–20, 31].

The maximum packing fraction marked as Φ_{mpc} is assumed to be 0.64 due to the irregular shape of the hybrid filler particles, while A is a parameter which depends on the shape of the particles. In this study we assumed $A = 5$ due to the high aspect ratio (i.e. particle length/wide) [20]. Our results show that the Lewis–Nielsen (2-phase) and modified Lewis–Nielsen (3-phase) approach give very close values. It can be evaluated that addition of second filler content at a constant and relatively low (5 wt%) level affected such result.

There are some other essential parameters of wide applicability, i.e., diffusivity d (m^2/s), effusivity e ($W\ s^{1/2}/(m^2\ K)$), specific heat c_p, and coefficient of thermal expansion (CTE) [32]. To describe the thermal behavior of a material one can use the thermal diffusivity

$$d = \frac{\lambda}{\rho c_p}, \tag{4}$$

as well as effusivity

$$e = (\lambda \rho c_p)^{1/2}, \tag{5}$$

where ρ (kg/m^3) is the bulk density. The coefficient λ ($W/(m\ K)$) is the thermal conductivity, and can be expressed with respect to d and e as $\lambda \sim e d^{1/2}$ [32, 33]. Calculated values of thermal effusivity and diffusivity are shown in Fig. 5 for both C/P [34] and C/G/P composites. The effusivity values of C/P composites are higher than that of C/G/P composites. Effusivity and diffusivity of composite materials increase with increasing Cu filler content. In the second portion of experiments, the sieved filler particles, as specified in experimental section, were tested at ten different mesh-size groups. The purpose was to investigate the effect of filler particle size on the variation of λ. The experiments were carried out at a constant concentration of 43% of Cu which is the volumetric concentration with the best efficiency of the composite electrode used in EDM (i.e., the higher material removal rate and the lower tool wear ratio) (see [22] for more information). The variation between particle size s and λ is given in Fig. 6.

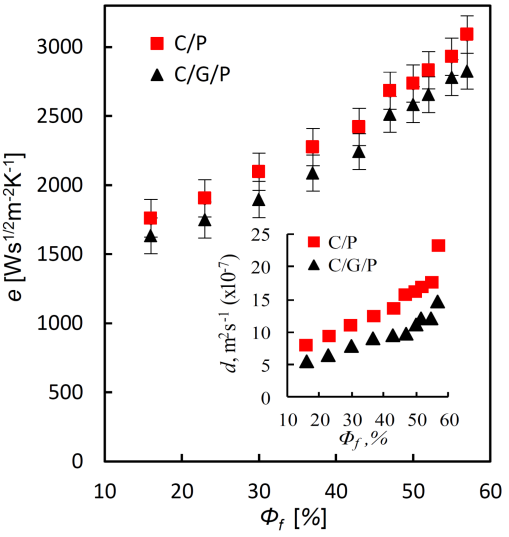

Fig. 5. The variation of effusivity and diffusivity of C/P and C/G/P composites with Cu % content.

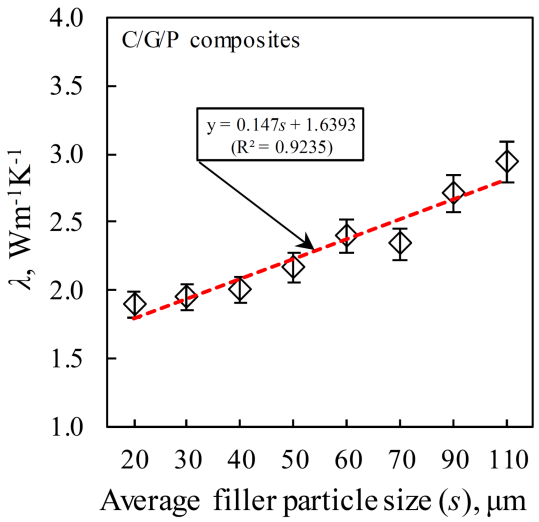

Fig. 6. The variation of λ with Cu filler size for C/G/P composites.

The growth of particle size increases the λ or results in a lower thermal resistivity. As the particle size is reduced, the polymer matrix encapsulates particles more easily due to the large interfacial area [35] and interrupts the mechanical contact between them. Therefore, more isolated particles cause lower λ values. The relationship between particle size s and λ under constant concentration (43%) is given in Fig. 6. In the study of Chen et al. [35] (Sect. 7.3), a similar result is presented in "size effect". The smaller filler size reduced the phonon transport because of the higher interfacial area of the filler.

3.3. Coefficient of thermal expansion

Polymers usually have CTEs up to 6 or 7 times higher than that of metals and ceramics. For this reason, the change in temperature during operation can reveal deformation differences that cause internal stresses at the interfaces [36]. These stresses can ultimately increase fracture, which leads to unwanted interface failure. For this reason, technologically, it is not enough to know the CTE value of a material. Thus, it is important to be able to adjust the value to the desired magnitude if possible.

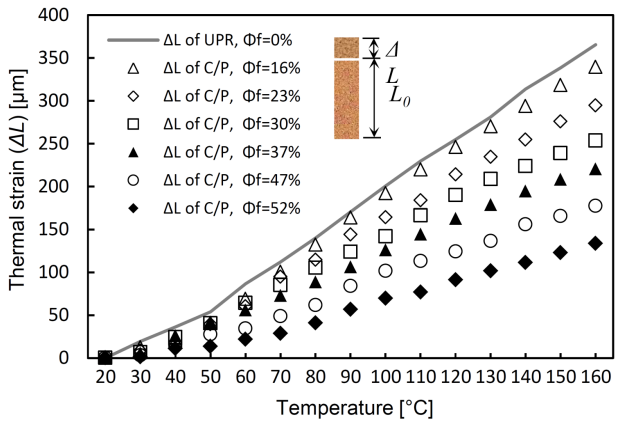

Fig. 7. Variation of longitudinal expansion of C/P composite vs. temperature.

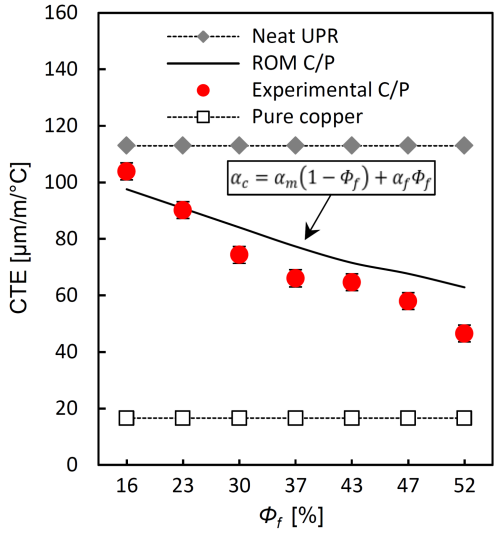

Fig. 8. Change of experimental and ROM CTE of C/P composites vs. % Cu.

In the present work, the CTE of the material is measured using a dilatometer instrument in a range of ±2500 μm. The composite samples are heated from room temperature up to 160 °C at a rate of 5 °C per min and measurements are taken. The CTEs are determined from the slope of the plot at 60 °C and 150 °C, showing the variation in size and temperature. The variation of thermal strain versus temperature change is given in Fig. 7.

At the same temperature condition, as the amount of filler added to the composite mixture increases, the thermal elongation values in the sample decrease. However, as the temperature increases in all different filler contents, the thermal expansion increases linearly. Metal powders which are dispersed in the polymer matrix and whose expansion coefficient is 6 times lower than that of the polymer material, inhibit the elongation of the polymer matrix as the temperature increases. There is a general trend towards the exploitation of using thermal expansion of Cu-containing composites [33, 37]. As shown in Fig. 8, the coefficient of thermal expansion decreases with the increasing concentration for materials containing Cu fillers, since the CTE of filler is much lower than that of polymer.

The CTE equation for composite materials according to rule of mixture (ROM) is given as

$$\alpha_c = \alpha_m (1 - \Phi_f) + \alpha_f \Phi_f, \tag{6}$$

where α_c, α_m, and α_f represent the CTE of the composite, of the matrix, and of the filler, respectively, and Φ_f is the volumetric concentration of filler. Since above equation was derived only for primary systems, so in this section C/P composite specimens were used in both, experimental and theoretical investigations. Equation (6) is used to estimate an approximate value, but it does not account for the distribution of fillers and interface interaction [36, 38]. The addition of filler also physically limits the polymer chains so that the overall expansion of the composite is reduced. Thus, after adding the larger quantities of the filler, the granules located between the polymer chains become tightened. This excessive compression reduces thermal expansion. Factors that can affect the degree of limitation, are filler size or aspect ratio, bulk modulus, and the distribution of filler particles in the matrix. As one can see in Fig. 8, the CTE of the filler is lower than that of the polymer matrix alone, and higher than the pure filler. The CTE of Cu is 16.6 μm/ °C [39]. This result indicates that incorporation of Cu particles into the epoxy matrix decreased the CTE of the composites [19, 36–38].

3.4. Density

Density measurements of C/P composite specimens allowed to calculate specific heat and λ. In this work, density measurements were made for cylindrical specimens (6 mm in diameter and 10 mm in height) with a Mettler-Toledo AT61 delta-range balance according to the gravity gage principle. Thus, one can use the density of the liquid to make calculation of the volume and specific mass of the sample easier. In addition, the density of composites with filler volumetric concentration relation can be written, according to Mamunya et al. [40], as

$$\rho_c = \rho_m (1 - \Phi_f) + \Phi_f \rho_f, \tag{7}$$

where ρ_c, ρ_f and ρ_m are the densities of composite, of the filler, and of the matrix, respectively, while Φ_f is the volumetric concentration of filler. Substituting values in (7), one can obtain the variation of the density of the C/P composite material with respect to the volumetric concentration of the added filler material. This change is shown in Fig. 9. We have investigated the effect of filler loading on the density for polymer composites. The density of the composites increases as filler loading increases.

The Cu particle as a pure metal, has a higher density than the pure resin. Therefore, increasing the filler content would increase the density of the composites. The same results can be seen in [39, 41]. In this work, the densities of pure Cu and UPR are taken as 8930 kg/m^3 and 1200 kg/m^3, respectively [22].

3.5. Specific heat

Specific heat or capacity of heat is a macroscopic thermodynamic property that is based on the degrees of freedom of the elementary components (molecules or atoms) of a material [42]. In this study, values of specific heat were determined experimentally using calorimetric measurement. The tests were carried out by using a Perkin Elmer Pyris Diamond DSC type scanning calorimeter (with $\pm\frac{1\%}{1\%}\ \frac{\text{accuracy}}{\text{precision}}$) under nitrogen atmosphere at a flow rate of 20 ml/min.

Calorimetric scans of the samples were made at a rate of 10 °C/min starting from temperature of 45 °C up to 160 °C, and kept isothermally for 3 min at the end of each scan. The results obtained are tabulated in Table III with volumetric filler contents and corresponding weight fractions. In Fig. 10, the specific heat shows approximately a horizontal trend between 50–150 °C temperature interval. When the concentration of filler increases within the composite mixture, the specific heat decreases.

For instance, the volumetric concentration shows a decrease in specific heat from about 0.9 to 0.4 (10^3 J/(kg °C)) at $\Phi_f = 16\%$ and at $\Phi_f = 50\%$ filler concentrations, respectively. This behavior can be explained by increasing the concentration of metal powders in the resin, which have a much lower specific heat value than neat resin [42–43]. In a homogeneous body, the thermal diffusivity d and λ are inter-related with each other by density ρ and specific heat c_p. The general relation is [33, 44–46]:

$$c_p = \frac{\lambda}{d\rho}. \tag{8}$$

According to ROM one can compute the theoretical c_{pc} values. Thus, we considered a 2-phase system and used specific heat values of pure matrix ($c_{pm} = 1200$ J/(kg K)) and pure Cu particles ($c_{pf} = 385$ J/(kg K))) [47]. The weight content-based ROM equations that we derived, were [47]:

$$c_{pc} = \frac{c_{p\ \text{total}}}{wt_{\text{total}}} = \frac{c_{pm} + c_{pf}}{wt_{\text{total}}} = \frac{c_{pm} wt_m + c_{pf} wt_f}{wt_{\text{total}}}, \tag{9}$$

$$c_{pc} = c_{pm}\,\Psi_m + c_{pf}\,\Psi_f, \tag{10}$$

where $\Psi_m = (wt_m/wt_{\text{total}})$ and $\Psi_f = (wt_f/wt_{\text{total}})$, and wt_m, wt_f are weight contents of matrix and filler materials, respectively. The summation of wt_m and wt_f is denoted by wt_{total}. The ROM values of specific heat based on the weight content are the lowest compared to the others (Fig. 11).

In Fig. 11 the specific heat decreases by increasing the weight content ($\text{wt}_\text{f}\%$) of filler. The theoretical c_p values calculated according to the ROM are slightly lower than that of the experimental values. However, the calculated specific heat values obtained from experimental λ and diffusivity are slightly lower than that of the experimental results. A similar situation has been reported in the literature [42, 43].

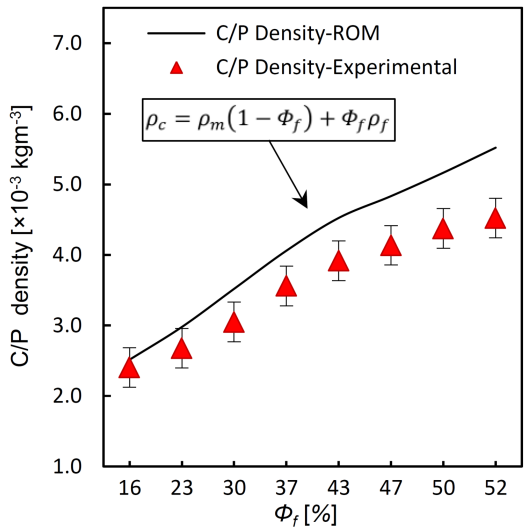

Fig. 9. Experimental and ROM density variation with volumetric concentration of C/P.

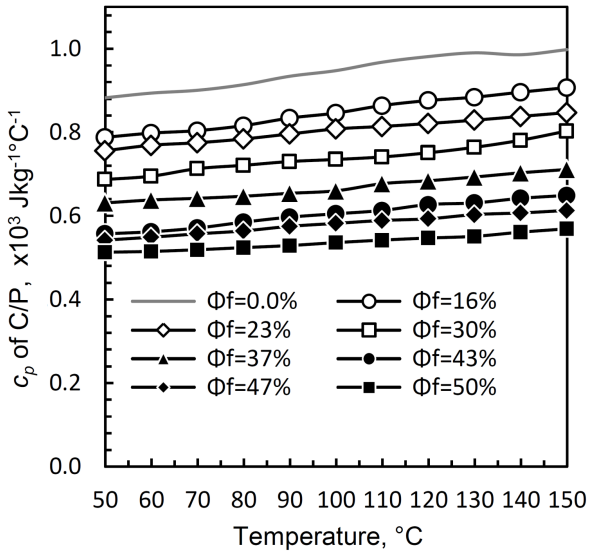

Fig. 10. Specific heat variation vs. temperature during heating stage for different % content of C/P composite.

TABLE III

Experimental, ROM and calculated c_p of C/P composites vs. % Cu.

Φ_f [%]	wt_f [%]	c_p ($\times 10^3$) [J/(kg °C)]		
		Exp.	ROM	Calc.
16	58	0.846	0.504	0.781
23	66	0.803	0.408	0.663
30	74	0.738	0.312	0.570
37	77	0.667	0.276	0.503
43	81	0.603	0.252	0.459
47	83	0.579	0.228	0.443
50	85	0.536	0.180	0.417
52	87	0.512	0.156	0.395

3.6. Electrical conductivity σ

In conductive metal filler–polymer composite systems, electrical conductivity increases as the concentration of the conductive filler increases [12, 26, 29, 33, 39, 40]. The growth is noticeably accelerated after a certain base concentration. This threshold concentration is called percolation. It is reported in the literature that the value of percolation concentration depends primarily on the concentration, shape and size of the filler used [22, 27, 34, 37, 38, 40]. Besides, the regular spatial distribution of conductive particles in the matrix, the amount of filler that should be added is of sufficient quantity and the physical properties of the polymer used are basic parameters that are effective on the percolation value. The curing temperature and duration, the mixing speed and time, the amount of catalyst and the accelerator used during the pre-curing and post-curing processes are secondarily influent [22, 40–42, 48]. In general, the electrical conductivity according to the percolation theory [1, 9, 22, 34, 40, 42] is given by

$$\sigma = \sigma(\Phi_f - \Phi_c)^t, \tag{11}$$

where σ_0 is the conductivity of the conducting phase, Φ_f is the concentration of the beginning of the conduction, Φ_c is the critical concentration, and t is the exponent of the conductivity. Expression (11) is used only for the threshold concentration Φ_c. In the vast majority of studies carried out in the literature, it is reported that σ is primarily dependent on the concentration of the conductive filler. On the other hand, studies on the effect of particle size are more limited relative to concentration. The common result of this limited number of studies is that the σ values increase as the particle size increases [22, 33, 36, 40, 41]. In Fig. 12, it is seen obviously that filler grain size increases approximately in direct proportion to the logarithmic conductivity. In the small graph attached to Fig. 12, the σ of composite samples of C/P and C/G/P type are given by logarithmic scale. C/P type composite samples have better conductivity than C/G/P. The percolation concentration for C/P samples is about 20%, while for C/G/P samples it is about 27%. According to the result, it can be concluded that as the electrical conductivity decreases, the filler threshold value increases as well.

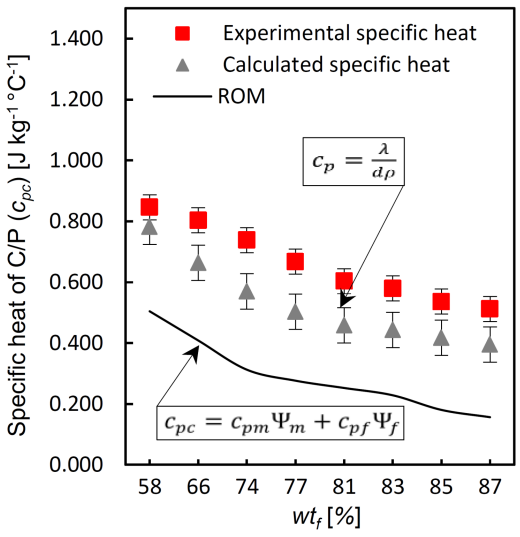

Fig. 11. Theoretical and experimental specific heat of C/P composite vs. Cu wt% content.

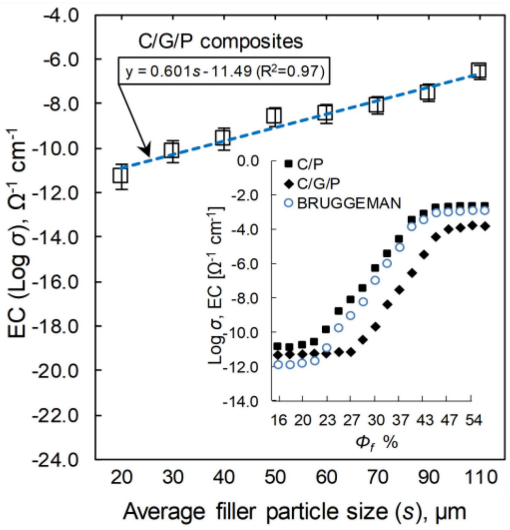

Fig. 12. The variation of σ with Cu filler size s of C/G/P and Φ_f effect on σ for both C/P, C/G/P composites and the comparison of the Bruggeman theoretical model.

According to the Bruggeman symmetrical effective medium theory [21] in a multi-phase (two or more types of inclusion) component medium, the following relation applies:

$$\sum \delta_i \frac{\sigma_i - \sigma_c}{\sigma_{fi} + 2\sigma_c} = 0, \tag{12}$$

where $i \in \{1, 2\}$, σ_{fi} is the i-th component electrical conductivity (σ_{f1} for filler1 and σ_{f2} for filler2), δ_i is the i-th component conductivity constant and σ_c is the EC of composite mixture. For 3-phase (two conductive filler) system the general equation can be simplified to

$$\delta_1 \frac{\sigma_{f1} - \sigma_c}{\sigma_{f1} + 2\sigma_c} + \delta_2 \frac{\sigma_{f2} - \sigma_c}{\sigma_{f2} + 2\sigma_c} = 0. \tag{13}$$

Equation (13) is a quadratic equation with respect to σ_c, whose positive solution is

$$\sigma_c = \frac{1}{4}\left(\gamma + \sqrt{\gamma^2 + 8\sigma_{f1}\sigma_{f2}}\right), \tag{14}$$

where

$$\gamma = (3\delta_2 - 1)\,\sigma_{f2} + (3\delta_1 - 1)\,\sigma_{f1}. \tag{15}$$

If Eq. (15) is calculated and the obtained values are substituted into (14) according to the theoretical model, then EC values of the composite structure can be yielded. The comparison between the calculated theoretical and experimental values are shown in the small graph inside Fig. 12. The calculated EC values are relatively bigger than experimental values of 3-phase structure, but give

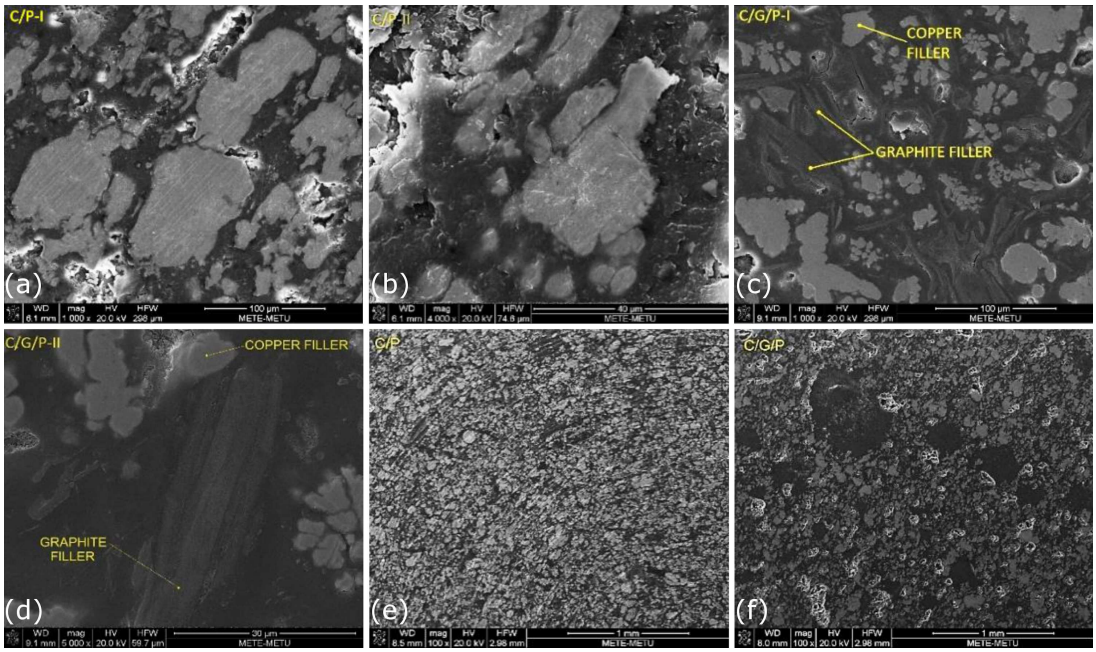

Fig. 13. SEM images (a), (b), and (e) for 86 wt%Cu-UPR and (c), (d), and (f) for 70 wt%Cu–5 wt%Gr–UPR hybrid composite with different magnifications.

closer values to 2-phase values. On the other hand, it gives lower values based on the experimental structures in the region where filler content is less than 20%. In these calculations when δ_1 and δ_2 values are taken as 1, the results closest to the experimental ones are achieved.

Conductivity values for the concentrations reached by saturation of the composite mixture are measured as about 10^{-4} and 10^{-2} Ω^{-1} cm^{-1} for C/P and C/G/P samples, respectively. The SEM images of 86 wt% of C/P composites are given in Fig. 13a, b, e and C/G/P (70 wt% Cu/5 wt% Gr-polyester) and hybrid composites are given in Fig. 13c, d, f. From the SEM images, the Cu and Gr particle dispersion can be observed in cured UPR media. In Fig. 13c, d, f the Gr particles scattered between the Cu particles are clearly visible in the SEM images.

The addition of 5 wt% Gr particle has very dense structural bridges among the Cu particles in the matrix. This hybrid filler-effect enhances the thermal insulation and violates the σ of the composite mixture. In Fig. 13c and Fig. 13d, the Gr particles, whose σ is much lower than the σ of Cu, did not give the expected synergy due to disruption in the conductivity network by prevention of direct contact with the Cu particles. The samples obtained by mixing Cu filler with UPR give very high σ values compared to the matrix alone. Since this composite material has high level of σ [22], it is used as an electrode for machining steel material by a die-sinker electro-erosion machine (EDM) successfully.

In work [22], authors compared the σ of their novel electrode with the spherical shaped Cu filler electrode produced by the same procedure. It was found out that the spherical electrodes had much lower electrical conductivities than dendritic ones. Considering this, it can be said that the dendritic structure presents much better conductivity results than the spherical structure because of the bigger contact surface area between filler particles. Using this high conductive polymeric novel composite material, very hard steel parts can be engraved. Composite electrode (top) and engraved steel work part (bottom) are shown in Fig. 14.

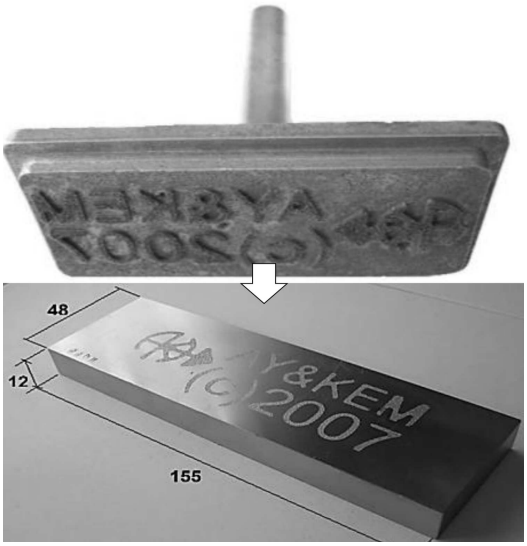

Fig. 14. Electrode (top) and machined SAE 1040 steel part (bottom) produced from a C/P composite in EDM [22].

4. Conclusion

This work presents experimental and theoretical studies on the thermal λ and electrical σ conductivities of a polymeric composite formed by combining two different fillers, namely Cu and Gr, with UPR binding. Experiments show that the λ and σ of the composite materials are increased by the Cu concentration. Especially, the C/P samples exhibit better conductivity behavior than their hybrid C/G/P counterparts. The highest λ value in C/P type samples was measured as 4.72 W/(m K). Adding Cu/Gr into the UPR increases the λ of the pure resin by about 20 times. The experimental results obtained are compared with some important theoretical models. Within these models, the closest λ results were obtained by the Maxwell model. For hybrid system, modified Lewis–Nielsen's model and Bruggeman's theoretical model give close values with the experimental results in TC and EC simulations, respectively. Thermal tests show that the thermal stability increases with the increasing Cu filler concentration. In the thermal analysis, the composite mixture has a major degradation at the temperature interval of 300–400 °C and the maximum weight loss is obtained at about the interval of 13–25% compared to neat resin. On the other hand, for all different filler content, the thermal expansion increases linearly with increasing temperature. In contrast, the thermal expansion decreases with increasing amount of filler added. The specific heat values exhibit the similar behavior with the λ's and the filler particle size has a positive effect on increasing in both λ and σ, so the larger particle size allows for a relatively higher conductive characteristic. Considering the mechanical performance, the hybrid effect allows positive contribution to the proposed composite structure.

References

[1] W. Zhou, J. Zuo, W. Ren, *Composites A* **43**, 658 (2012).

[2] A. Agrawal, A. Satapathy, *Proced. Eng.* **51**, 573 (2013).

[3] W.C. Choi, K.H. Yoon, S.S. Jeong, *Composites A* **45**, 1(2013).

[4] P.G. Ren, X.H. Si, Z.F. Sun, F. Ren, L. Pei, S.Y. Hou, *J. Polym. Res.* **23**, 21 (2016).

[5] F.Y. Yuan, H.B. Zhang, X. Li, X.Z. Li, Z.Z. Yu, *Composites A* **53**, 137 (2013).

[6] J. Yu, H.K. Choi, H.S. Kim, S.Y. Kim, *Composites A* **88**, 79 (2016).

[7] H. Zhang, G. Zhang, M. Tang, L. Zhou, J. Li, X. Fun, X. Shi, J. Qin, *Chem. Eng. J.* **353**, 381 (2018).

[8] T.K.B. Sharmila, J.V. Antony, M.P. Jayakrishnan, P.M.S. Beegum, E.T. Thachill, *Mater. Des.* **90**, 66 (2016).

[9] C. Pan, K. Kou, Y. Zhang, Z. Li, G. Wu, *Composites B* **153**, 1 (2018).

[10] I.L. Ngo, S. Jeon, C. Byon, *Int. J. Heat Mass Transf.* **98**, 219 (2016).

[11] D.C. Moreira, L.A. Sphaier, J.M.L. Reis, L.C.S. Nunes, *Exp. Therm. Fluid Sci.* **35**, 1458 (2011).

[12] I. Krupa, V. Cecen, A. Boudenne, J. Prokes, I. Novak, *Mater. Des.* **51**, 620 (2013).

[13] M. Shen, Y. Cui, J. He, Y. Zhang, *Int. J. Min. Met. Mater.* **18**, 623 (2011).

[14] L. Kowalski, J. Duszczyk, L. Katgerman, *J. Mater. Sci.* **34**, 1 (1999).

[15] F. Danes, B. Garnier, T. Dupuis, *Int. J. Thermophys.* **24**, 771 (2003).

[16] K. Pietrak, T.S. Wisniewski, *J. Power Technol.* **95**, 14 (2015).

[17] I.H. Tavman, *Powder Technol.* **91**, 63 (1997).

[18] A. Tessema, D. Zhao, J. Moll, S. Xu, R. Yang, C. Li, S.K. Kumar, A. Kidane, *Polym. Test.* **57**, 101 (2017).

[19] A. Badakhsh, C.W. Park, *J. Appl. Polym.* **134**, 45397 (2017).

[20] Y.S. Perets, L.L. Vovchenko, L.Y. Matzui, A. Zhuravkov, A.V. Trukhanov, O.A. Lazarenko, *Mat. Werkstofftech* **47**, 278 (2016).

[21] R. Landauer, *AIP Conf. Proc.* **40**, 2 (1978).

[22] K. Yaman, C. Çogun, *Int. J. Adv. Manufact. Technol.* **73**, 535 (2014).

[23] A.R. Blythe, *Polym. Test.* **4**, 195 (1984).

[24] W. Guoquan, *Polym. Test.* **16**, 277 (1997).

[25] A.S. Luyt, J.A. Molefi, H. Krump, *Polym. Degrad. Stabil.* **91**, 1629 (2006).

[26] C. Bora, P. Bharali, S. Baglari, S.K. Dolui, B.K. Konwar, *Composit. Sci. Technol.* **87**, 1 (2013).

[27] V. Cecen, Y. Seki, M. Sarikanat, I.H. Tavman, *J. Appl. Polym. Sci.* **108**, 2163 (2008).

[28] A. Ansari, M.J. Akhtar, *R.S.C. Adv.* **6**, 13846 (2016).

[29] B. Biswas, S. Chabri, B.C. Mitra, K. Das, N.R. Bandyopadhyay, A. Sinha, *J. Inst. Eng. Ind. Ser. D* (2016).

[30] K. Gaska, A. Rybak, C. Kapusta, R. Sekula, A. Siwek, *Polym. Adv. Technol.* **26**, 26 (2014).

[31] H. Song, B.G. Kim, Y.S. Kim, Y.S. Bae, J. Kim, Y. Yoo, *Polymers* **11**, 484 (2019).

[32] T.A. El-Brolossy, S.S. Ibrahim, *Thermochim. Acta* **509**, 46 (2010).

[33] A. Boudenne, L. Ibos, M. Fois, J.C. Majeste, E. Gehin, *Composites A* **36**, 1545 (2005).

[34] K. Yaman, Ö. Taga, *Int. J. Polym. Sci.* (2018).

[35] H. Chen, V.V. Ginzburg, J. Yang, Y. Yang, W. Liu, Y. Huang, L. Du, B. Chen, *Prog. Polym. Sci.* **59**, 41 (2016).

[36] J.G. Benito, E. Castillo, J.F. Caldito, *Europ. Polym. J.* **49**, 1747 (2013).

[37] R.K. Goyal, K.R. Kambale, S.S. Nene, B.S. Selukar, S. Arbuj, U.P. Mulik, *Mater. Chem. Phys.* **128**, 114 (2011).

[38] T.K. Dey, M. Tripathi, *Thermochim. Acta* **502**, 35 (2010).

[39] M.N.F. Pargi, T.P. Leng, S. Husseinsyah, C.K. Yeoh, *Polym.-Plast. Technol. Eng.* **54**, 265 (2015).

[40] Y.P. Mamunya, V.V. Davydenko, P. Pissis, E.V. Lebedev, *Europ. Polym. J.* **38**, 1887 (2002).

[41] A. Agrawal, A. Satapathy, *Composites A* **63**, 51 (2014).

[42] T. Osswald, J.P.H. Ortiz, *Polymer Processing*, Hanser Pub., Cincinnati 2008.

[43] L. Riviere, N. Causse, A. Lonjon, E. Dantras, C. Lacabanne, *Polym. Degrad. Stab.* **127**, 98 (2016).

[44] R. Tlili, A. Boudenne, V. Cecen, L. Ibos, I. Krupa, Y. Candau, *Int. J. Thermophys.* **31**, 936 (2010).

[45] D. Ratna, *Thermal Properties of Thermosets* in: *Thermosets Structure, Properties and Applications* Ed. Qipeng Guo, Woodhead, 2012, p. 62.

[46] B. Weidenfeller, M. Höfer, F.R. Schilling, *Composites A* **35**, 423 (2004).

[47] Matmatch.com, *General Unsaturated Polyester/Type 802*.

[48] A. Boudenne, Y. Mamunya, V. Levchenko, B. Garnier, E. Lebedev, *Europ. Polym. J.* **63**, 11 (2015).